

Bullen's parameter as a seismic observable for spin crossovers in the lower mantle

Juan J. Valencia-Cardona¹, Quentin Williams², Gaurav Shukla³, Renata M.

Wentzcovitch^{4,5}

arXiv:1707.08636v1 [physics.geo-ph] 26 Jul 2017

Corresponding author: Juan J. Valencia-Cardona, Scientific Computing Program, University of Minnesota, Minneapolis, Minnesota, USA. (valen167@umn.edu)

¹Scientific Computing Program,
University of Minnesota, Minneapolis,
Minnesota, USA

²Department of Earth and Planetary
Sciences, University of California Santa
Cruz, Santa Cruz, California, USA

³Department of Earth, Ocean, and
Atmospheric Science, Florida State
University, Tallahassee, Florida, USA

⁴Department of Applied Physics and
Applied Mathematics, Columbia University,
New York City, New York, USA

⁵Lamont-Doherty Earth Observatory,
Columbia University, Palisades, New York,
USA

Elastic anomalies produced by the spin crossover in ferropericlasite have been documented by both first principles calculations and high pressure-temperature experiments. The predicted signature of this spin crossover in the lower mantle is, however, subtle and difficult to geophysically observe within the mantle. Indeed, global seismic anomalies associated with spin transitions have not yet been recognized in seismologic studies of the deep mantle. A sensitive seismic parameter is needed to determine the presence and amplitude of such a spin crossover signature. The effects of spin crossovers on Bullen's parameter, η , are assessed here for a range of compositions, thermal profiles, and lateral variations in temperature within the lower mantle. Velocity anomalies associated with the spin crossover in ferropericlasite span a depth range near 1,000 km for typical mantle temperatures. Positive excursions of Bullen's parameter with a maximum amplitude of ~ 0.03 are calculated to be present over a broad depth range within the mid-to-deep lower mantle: these are largest for peridotitic and harzburgitic compositions. These excursions are highest in amplitude for model lower mantles with large lateral thermal variations, and with cold downwellings having longer lateral length-scales relative to hot upwellings. We conclude that predicted deviations in Bullen's parameter due to the spin crossover in ferropericlasite for geophysically relevant compositions may be sufficiently large to resolve in accurate seismic inversions of this parameter, and could shed light on both the lateral variations in temperature at depth within the lower mantle, and the amount of ferropericlasite at depth.

1. Introduction

The adiabatic nature of the convecting mantle is a frequently used concept in the geophysical sciences. For instance, equation of state parameters, which are used to calculate the elastic and thermodynamic properties of minerals at mantle conditions, are commonly assumed to be adiabatic within the convecting mantle, e.g., the adiabatic bulk modulus and its derivative. However, various geodynamic simulations and seismological models [Bunge *et al.*, 2001; Dziewonski and Anderson, 1981; Kennett *et al.*, 1995; Mattern *et al.*, 2005; Matyska and Yuen, 2000, 2002] suggest that the mantle is regionally nonadiabatic, particularly in the shallow and deep mantle regions, and in some cases, at mid lower mantle pressures. The latter is important because deviations from adiabaticity within the mantle provide insights into temperature gradients, heat flux, thermal history, thermal boundary layers, phase transitions, chemical stratification, and compositional heterogeneities. Therefore, knowledge about the degree of adiabaticity of the mantle helps us to constrain its composition and thermal structures related to mantle convection [Matyska and Yuen, 2000].

A common observable that quantifies the adiabaticity level of the mantle is Bullen's parameter, η . Introduced and developed by Bullen [1949, 1963], η is a measure of the ratio between the actual density increase with pressure within the Earth (as constrained by a combination of seismology, the Earth's moment of inertia, and mass) with respect to the profile derived from adiabatic self-compression. As such, it is expected to be unity where the mantle is homogeneous, adiabatic, and free of phase transitions. Thus, deviations of η from unity (generally $\sim \pm 0.1$ or less), indicate super(sub)adiabatic regions, and

consequently, the presence of thermal boundary layers, compositional variations or phase transitions. Moreover, there is also the possibility that due to internal heating within the mantle, the mantle may be systematically subadiabatic [*Bunge et al.*, 2001].

Evaluations of η in geodynamic simulations are generally done by probing the parameter space associated with plausible convection models. This includes examining the effects of possible variations of the thermal conductivity, thermal expansion coefficient, viscosity, internal heating, and heat flux from the core, each of which directly impact the inferred geotherms [*Bunge et al.*, 2001; *Matyska and Yuen*, 2000, 2002]. For instance, if internal heating is relatively significant, subadiabaticity is expected. Additionally, differences in elastic properties between individual phases within an aggregate can also produce variations in Bullen's parameter, and hence apparent deviations from adiabaticity. This is a bulk attenuation effect. Specifically, bulk attenuation phenomena are attributed to internal shear stresses generated from the local mismatch of the elastic moduli of neighboring grains in a given aggregate. One formulation of bulk attenuation by *Heinz et al.* [1982] characterizes it through the ratio of the adiabatic bulk modulus K_S and an effective modulus (Reuss bound) K_E , since the mantle can be assumed to be under hydrostatic pressure. Attenuation is a complicated problem to tackle, because it involves calculating complex moduli with an associated time dependency [*Heinz et al.*, 1982; *Heinz and Jeanloz*, 1983; *Budiansky et al.*, 1983]. Such bulk attenuation effects are beyond the scope of this study, since the calculations we conduct are not time-dependent, but certainly needs to be addressed to understand systematic deviations of Bullen's parameter from 1. Here, we study

how anomalies in bulk modulus induced by spin crossovers affect the Bullen's parameter, and hence inferred adiabaticity of the lower mantle.

Elastic anomalies produced by the spin crossover in ferropericlase (fp) and bridgmanite (bdg), have been documented by both first principles calculations and high pressure-temperature experiments [*Badro et al.*, 2003; *Speziale et al.*, 2005; *Tsuchiya et al.*, 2006; *Wentzcovitch et al.*, 2009; *Wu et al.*, 2009; *Crowhurst et al.*, 2008; *Marquardt et al.*, 2009; *Antonangeli et al.*, 2011; *Murakami et al.*, 2012; *Wu et al.*, 2013; *Wu and Wentzcovitch*, 2014; *Hsu et al.*, 2011, 2012; *Shukla et al.*, 2016; *Shukla and Wentzcovitch*, 2016]. The predicted signatures of this spin crossover in the lower mantle are subtle. Despite the fact that thermally induced velocity heterogeneities associated with this spin crossover appear to correlate statistically with seismic tomographic patterns observed in deeply rooted plumes [*Wu and Wentzcovitch*, 2014], spherically averaged anomalies have not yet been recognized in seismologic studies of the deep mantle. This may be due to difficulties associated with resolving gradual changes in the slopes of seismic velocities as a function of depth, and the trade-offs involved in seismic inversions of depth-dependent velocity and density structures. In particular, velocity anomalies associated with the spin crossover in fp are anticipated to span a depth range greater than 1000 km at mantle temperatures. Thus, a sensitive seismic parameter is needed to determine the presence or absence of this spin crossover signature, which would in turn shed light on the amount of ferropericlase in the lower mantle. Bullen's parameter η is an ideal candidate as it relates seismic wave speeds with density variations, and sensitively records deviations from adiabaticity. Moreover, deviations from Bullen's parameter can be readily identified because it has a

clear reference value (unity) in an adiabatic mantle that is heated from below. We calculated one dimensional perturbations of η due to changes in composition, temperature, and spin crossover. We achieved this by computing η of different relevant mantle aggregates along their own adiabats. We also approximate lateral variations in temperature by modeling differing areas and temperature differences between upwellings and downwellings. The mantle phases of the aggregates considered are bridgmanite (bdg: Al-Fe-bearing MgSiO_3 perovskite), CaSiO_3 perovskite (CaPv), and ferropericlasite (fp: $(\text{Mg,Fe})\text{O}$). The aggregates have Mg/Si ratios that range from 0.82 to 1.56 and are harzburgite (Mg/Si \sim 1.56) [Baker and Beckett, 1999], chondrite (Mg/Si \sim 1.07) [Hart and Zindler, 1986], pyrolite (Mg/Si \sim 1.24) [McDonough and Sun, 1995], peridotite (Mg/Si \sim 1.30) [Hirose and Kushiro, 1993], and perovskite only (Mg/Si \sim 0.82) [Williams and Knittle, 2005]. The predicted deviations in η due to the spin crossover are comparable to previously reported variations [Bunge et al., 2001; Matyska and Yuen, 2000, 2002; Mattern et al., 2005], and may be sufficiently large to turn up in accurate seismic inversions of this parameter.

2. Method and Calculation Details

We used bdg $\text{Mg}_{1-x}\text{Fe}_x^{2+}\text{SiO}_3$, $(\text{Mg}_{1-x}\text{Al}_x)(\text{Si}_{1-x}\text{Al}_x)\text{O}_3$, $(\text{Mg}_{1-x}\text{Fe}_x^{3+})(\text{Si}_{1-x}\text{Al}_x)\text{O}_3$, $(\text{Mg}_{1-x}\text{Fe}_x^{3+})(\text{Si}_{1-x}\text{Fe}_x^{3+})\text{O}_3$ ($x = 0$ and 0.125) and fp $\text{Mg}_{1-y}\text{Fe}_y\text{O}$ ($y = 0$ and 0.1875) thermoelastic properties from Shukla et al. [2015, 2016] and Wu et al. [2013]. Results for other x and y values were obtained by linear interpolation. All compositions account for the spin crossover in fp unless otherwise noted, i.e., bdg's iron (ferrous and/or ferric) is in the high spin (HS) state and fp is in a mixed spin (MS) state of HS and low spin (LS) states. For CaPv, we used thermoelastic properties from Kawai and Tsuchiya [2014, 2015], which

were reproduced within the Mie-Debye-Grüneisen [*Stixrude and Lithgow-Bertelloni, 2005*] formalism. The mantle aggregates in this study, namely, harzburgite [*Baker and Beckett, 1999*], chondrite [*Hart and Zindler, 1986*], pyrolite [*McDonough and Sun, 1995*], peridotite [*Hirose and Kushiro, 1993*], and perovskitic only [*Williams and Knittle, 2005*], are mixtures within the SiO_2 - MgO - CaO - FeO - Al_2O_3 system (ignoring alkalis and TiO_2 is not anticipated to resolvably affect the results). In addition, the Fe-Mg partition coefficient $K_D = \frac{x/(1-x-z)}{y/(1-y)}$ between bdg and fp, which is known to be affected by the spin crossover [*Irifune et al., 2010; Piet et al., 2016*], was assumed to be uniform throughout the mantle with a value of 0.5. Further details about these compositions can be found in *Valencia-Cardona et al. [2017]*.

The adiabats of the different minerals and aggregates were integrated from their adiabatic gradient,

$$\left(\frac{\partial T}{\partial P}\right)_S = \frac{\alpha VT}{C_p} \quad (1)$$

We denote the molar fraction, molar volume, molar mass, thermal expansion coefficient, and isobaric specific heat of the i^{th} mineral in the mixture as μ_i , V_i , M_i , α_i , and C_{p_i} respectively. The aggregate properties such as volume, thermal expansion coefficient, and isobaric specific heat are then $V = \sum_i \mu_i V_i$, $\alpha = \sum_i \alpha_i \mu_i V_i / V$, and $C_p = \sum_i \mu_i C_{p_i}$. The adiabatic aggregate bulk moduli K_S were obtained from the Voigt-Reuss-Hill (VRH) average. Moreover, the aggregate density $\rho = \sum_i \mu_i M_i / V$ and seismic parameter $\phi = K_S / \rho$ were calculated along the aggregate adiabat, in order to compute adiabatic changes of density with respect to pressure as,

$$\eta = \phi \frac{d\rho}{dP} \quad (2)$$

where η is the Bullen's parameter. If $\eta = 1$ the mantle is homogeneous and adiabatic, whereas values of $\eta > 1$ can indicate a phase change as ρ varies more rapidly with depth than predicted by the adiabat. Furthermore, values of $\eta < 1$ may signify the presence of a thermal boundary layer or substantial internal heat production. Details about equation (2) can be found in the supplementary information.

3. Results and Discussion

3.1. Observations of η in the lower mantle

Figure 1 shows different η calculations from previous geodynamic [*Bunge et al.*, 2001; *Matyska and Yuen*, 2000, 2002], seismic [*Dziewonski et al.*, 1975; *Dziewonski and Anderson*, 1981; *Kennett et al.*, 1995], and seismic plus mineral physics models with a priori starting conditions [*Mattern et al.*, 2005]. Overall, η oscillates between values of ~ 1.04 to 0.96 for most of these models, except for the AK135F model [*Kennett et al.*, 1995; *Montagner and Kennett*, 1996], which displays the largest fluctuations. AK135F exhibited an average value of $\eta \sim 0.92$ from 1000 km to 2700 km in depth, and variations in η above and below those depths were at least of the order of ~ 0.1 , which is substantially larger than the other inversions and calculations. For other seismic models such as PEM [*Dziewonski et al.*, 1975] and PREM [*Dziewonski and Anderson*, 1981] such large fluctuations are not observed, but they could be suppressed by the continuity requirements of the polynomial formulations of these models. However, the Bullen's parameters of these seismic models do suggest the presence of a thermal boundary layer at the bottom of the lower mantle, as shown by the negative slope of all models in the bottommost hundred to few hundred km of the mantle. Notably, for the mineral physics plus inverse model calculation by *Mattern et al.* [2005], η values less than one from 800 km to 1300 km were attributed to iron depletion from their initially pyrolitic compositional model.

Two and three dimensional geodynamic calculations of η were first done by *Matyska and Yuen* [2000, 2002], where the effect of varying parameter space properties, such as thermal conductivity, thermal expansion coefficient, and viscosity, lead to different perturbations in η , but with an average value of ~ 1.01 . This average value is in general agreement with

other geodynamic calculations by *Bunge et al.* [2001], which also showed that the presence of internal heat sources lead to subadiabatic regions. Other thermal contributions, like core heating, cause superadiabatic temperature gradients at the bottom of the mantle and thus the presence of a thermal boundary layer, as manifested by the negative slopes of η near the base of the mantle.

3.2. Spin-crossover effect on the adiabaticity of the lower mantle

We studied the effect of spin crossovers on lower mantle adiabaticity by examining η excursions for different lower mantle aggregates along their self consistent adiabats. All of the adiabats of the different aggregates are listed in *Valencia-Cardona et al.* [2017]. Figure 2 shows the variations of η only due to the spin crossover in fp: only a portion of trivalent iron in bdg is anticipated to undergo a spin transition within the mantle (e.g., *Catalli et al.* [2010] and *Hsu et al.* [2011, 2012]). For compositions with fp, fluctuations in η were ~ 0.02 max, which are well within the variations in seismological observations and geodynamical calculations shown in Figure 1. Furthermore, larger deviations from adiabaticity occur as the aggregates Mg/Si ratio, i.e., fp content, is increased. The sensitivity to Mg/Si content of the Bullen's parameter maximum near 1900 km depth, induced by the spin crossover, is relatively large: peridotitic and harzburgitic compositions have an η anomaly which is nearly twice that of the chondritic composition. The η excursions for the perovskitic composition, Pv only, depict the profile of a composition without fp in the lower mantle.

3.3. Lateral temperature variations

We have characterized what Bullen parameter anomalies, due to spin crossovers, might generate for one-dimensional seismic models of an isochemical adiabatic mantle. However,

the lack of maxima in most Bullen parameter observations (Figure 1) that are at the appropriate depth and have the right breadth to correspond to the spin crossover of fp, led us to probe the effect of lateral temperature variations on deviations of η . Since lateral temperature variations and their areal distribution at a given depth of hot/upwelling and cold/downwelling material are not well-constrained in the deep mantle (e.g., *Houser and Williams* [2009]), we conducted a sensitivity analysis for the effect of thermal variations on η in a pyrolitic mantle. Here, material at each depth is distributed along adiabats with potential temperatures above (hot) and below (cold) a reference adiabat pinned at 1873 K at 23 GPa as in *Brown and Shankland* [1981] (B&S) (See also [*Akaogi and Akimoto*, 1979]). The lateral temperature variations between hot and cold regions that we probed were ± 250 K, ± 500 K, and ± 750 K in a sequence of 25%:75%, 50%:50% and 75%:25% ratio of the mantle at a given depth being hot:cold (See Figure 3).

For all the temperature-average distributions (Figures 3a, 3b, and 3c), we observed that the spin crossover anomalies, i.e. deviations from adiabaticity, became more prominent at lower temperatures: this is a natural consequence of the broadening of the spin transition that occurs at high temperatures. Conversely, greater amounts of hot material tend to make spin crossovers more difficult to resolve. Furthermore, we also observed that for large temperature variations, ± 750 K, two peaks in η can also be generated at different depths in an isochemical thermally heterogeneous mantle (Figure 3c). This phenomenon is attributed to the volume increase with temperature, which increases the pressures that are required for the spin crossover to occur. Since the amplitude of the perturbations in η increases also with higher fp content, it is expected that regions with larger cold

harzburgitic chemistry present within the lower mantle, such as subducting slabs, should have substantially greater local fluctuations in the Bullen's parameter if a local vertical sampling of η over such regions is performed.

Beyond lateral temperature variations, we examined the case of coupled compositional and thermal lateral heterogeneities. The rationale here is that cold, downwelling subducted material is likely to have a larger concentration of harzburgite than ambient mantle. We utilized a similar temperature averaging scheme, but with cold η values being harzburgitic. Figure 4 shows different η profiles with the mantle being 75% hot(pyrolite) and 25% cold(harzburgite). For this scenario, perturbations in η due to the spin crossover vary their magnitude and reach a maxima at different depths, depending on the temperature difference between the cold downwellings of harzburgitic chemistry and ambient pyrolitic mantle. If the temperature difference is sufficiently large, e.g. ± 750 K, multiple peaks can be observed. Thus, the relative amplitudes and locations of multiple peaks could, if observed/observable, provide strong constraints on lateral variations in the geotherm and/or composition of the deep mantle. In particular, the depth at which the spin transition-induced peak occurs in Bullen's parameter is highly sensitive to temperature (Figure 3), while the amplitude of its variation is sensitive to composition (Figure 2).

4. Geophysical Significance

We have utilized η as an observable for spin crossovers in the lower mantle for the first time, in an attempt to reconcile mineral physics with seismic observations and to understand how such spin crossovers may affect observations of deviations from adiabaticity

within the mantle. Our results suggest that the spin crossover signatures in η should be sufficiently large to turn up in accurate (ca. 1%) seismic inversions for this parameter. Whether such accuracies are achievable is unclear: several decades ago, *Masters* [1979] concluded that η variations from seismic observations could be resolved with a precision no better than 2%. Recent results from an inverse Bayesian method, deployed via a neural network technique by *De Wit and Trampert* [2015], showed that ρ , V_p , and V_s may each be resolvable to somewhat better than 1% in the ~ 2000 km depth range, based on their observed probability density functions. A linear combination of these uncertainties will certainly lead to values of order 1-2.5% for the net uncertainty in 1-D inversions for Bullen's parameter. Nevertheless, given markedly improved and more accurate seismic inversions coupled with substantially larger data sets, it is possible that better constraints on η might be developed.

We also highlight the importance of the chosen temperature profile, as it has a direct impact on η . Elastic moduli, seismic velocities, and aggregate densities strongly depend on temperature. Hence, super(sub)adiabatic geotherms will lead to different interpretations of η . As recently showed by *Valencia-Cardona et al.* [2017], the spin crossover in fp and bdg induces an increment in the adiabat's temperature of a given aggregate and such a temperature increment will impact η 's sensitivity. Because of the potentially complex coupling of lateral temperature differences with compositional variations, further work on the effect of spin crossovers on η would likely benefit from an assessment within a three dimensional convective scheme, such as the formulation proposed by *Matyska and Yuen* [2002].

5. Conclusions

Apparent deviations from adiabaticity due to spin crossover, as recorded by the Bullen's parameter, increased in proportion to the aggregate's ferropericlasite content. The magnitude of these perturbations is generally consistent with the magnitude of variations in η present in previous seismological and geodynamic inversions of η in the lower mantle. Our results provide a sense of how much of a perturbation in η , given the spin crossover and lateral temperature variations, might be expected in one dimensional seismic models, with the net result being of order 1-2%. Accurate characterization of η either globally or locally could provide constraints on both the lateral temperature distribution and the fp content at depth, although such determinations hinge critically on achieving sufficient seismic resolution to resolve spin transitions. Also, the perturbations found in η for different mantle temperature averages highlight the importance of doing vertical seismic velocity profiles with sufficient precision to allow η to be characterized on a regional basis. Our results provide a guide for possible a priori models of η in regionalized inversions of velocity as a function of depth: inversions without spin crossover induced perturbations in η implicitly assume that spin transitions are absent at depth, and hence that no ferropericlasite is present in the deep mantle.

Acknowledgments. We thank two reviewers for helpful comments. This work was supported primarily by grants NSF/EAR 1319368 and 1348066. Q. Williams was supported by NSF/EAR 1620423. Results produced in this study are available in the supporting information. The 2016 CIDER-II program (supported by NSF/EAR 1135452) is thanked for providing a portion of the original impetus of this study.

6. Supplementary Material

The supporting information consists of Text S1, Figure S1, and Table S1. Figure S1 shows η for prystine lower mantle minerals, namely, MgSiO_3 , MgO , and CaSiO_3 . Text S1 shows the Bullen's parameter η derivation. Table S1 the values of η for the different aggregates.

6.1. Text S1

The bulk modulus of a mineral under adiabatic self compression is given by,

$$K_S = \rho \left(\frac{\partial P}{\partial \rho} \right)_S \quad (3)$$

Hence,

$$\frac{K_S}{\rho} = \left(\frac{\partial P}{\partial \rho} \right)_S = \phi \quad (4)$$

where ϕ is the seismic parameter $\phi = V_P^2 - \left(\frac{4}{3}\right) V_S^2$.

Furthermore, assuming a homogeneous media under hydrostatic changes in pressures with respect to depth,

$$\frac{dP}{dr} = -\rho g \quad (5)$$

where g and r are the acceleration due gravity and depth, respectively.

Thus,

$$\frac{dP}{d\rho} \frac{d\rho}{dr} = -\rho g \quad (6)$$

and using equation (4),

$$1 = -\phi\rho^{-1}g^{-1}\frac{d\rho}{dr} \quad (7)$$

Equation (7) is known as the Adams-Williamson equation.

If the system is not adiabatic, i.e., equation (7) differs from the unity, we have,

$$\eta = -\phi\rho^{-1}g^{-1}\frac{d\rho}{dr} = \phi\frac{d\rho}{dP} \quad (8)$$

where η is the Bullen's parameter [*Bullen*, 1963].

References

- Akaogi M. and Akimoto S. (1979), High-pressure phase equilibria in a garnet lherzolite, with special reference to Mg^{2+} Fe^{2+} partitioning among constituent minerals, *PEPI*, *19*, 31–51.
- Antonangeli D., Siebert J., Aracne C.M., Farber D.L., Bosak A., Hoesch M., Krisch M., Ryerson F.J., Fiquet G. and Badro J. (2011), Spin crossover in ferropericlase at high pressure: a seismologically transparent transition?, *Science*, *331*, 64-67.
- Badro J., Fiquet G., Guyot F., Rueff J.P., Struzhkin V.V., Vank G. and Monaco G. (2003), Iron partitioning in Earth's mantle: toward a deep lower mantle discontinuity, *Science*, *300*, 789-791.
- Baker M.B., J.R. Beckett (1999), The origin of abyssal peridotites: a reinterpretation of constraints based on primary bulk compositions, *Earth Planet. Sci. Lett.*, *171*, 49-61.
- Bengtson A., Li J., and Morgan D. (2009), Mössbauer modeling to interpret the spin state of iron in (Mg, Fe)SiO₃ perovskite, *Geophys. Res. Lett.*, *36*, L15301, doi:

1029/2009GL038340.

Brown J.M. and T.J. Shankland (1981), Thermodynamic parameters in the Earth as determined from seismic profiles, *Geophys. J. R. astr. Soc.*, *66*, 579–596.

Budiansky B., Sumner E.E., and O'Connell R.J. (1983), Bulk thermoelastic attenuation of composite materials, *J. Geophys. Res. Solid Earth*, *88*, 10343-10348.

Bullen K.E. (1949), Compressibility-pressure hypothesis and the Earth's interior, *Geophysical Supplements to the Monthly Notices of the Royal Astronomical Society*, *5*, 335-368.

Bullen K.E. (1963), An index of degree of chemical inhomogeneity in the Earth, *Geophys. J. Inter.*, *7*, 584-592.

Bunge H.P., Ricard Y., and Matas J. (2001), Non-adiabaticity in mantle convection, *Geophys. Res. Lett.*, *28*, 879-882.

Catalli K., Shim S.H., Prakapenka V.B., Zhao J., Sturhahn W., Chow P., Xiao Y., Liu H., Cynn H. and Evans W.J. (2010), Spin state of ferric iron in MgSiO₃ perovskite and its effect on elastic properties, *EPSL*, *289*, 68-75.

Crowhurst, J.C., Brown, J.M., Goncharov, A.F. and Jacobsen, S.D. (2008), Elasticity of (Mg, Fe)O through the spin transition of iron in the lower mantle, *Science*, *319*, 451-453.

De Wit R.W.L. and Trampert J.(2015), Robust constraints on average radial lower mantle anisotropy and consequences for composition and texture, *EPSL*, *429*, 101-109.

Dziewonski A.M., A.L. Hales, and E.R. Lapwood. (1975), Parametrically simple earth models consistent with geophysical data, *Phys. Earth Planet. Int.*, *10*, 12-48.

- Dziewonski, A. M., and D. L. Anderson (1981), Preliminary reference Earth model, *Phys. Earth Planet. Int.*, *25*, 297–356.
- Hart S. R. and A. Zindler (1986), In search of a bulk-Earth composition, *Chem. Geo.*, *57*, 247–267, doi:10.1016/0009-2541(86)90053-7.
- Heinz D., Jeanloz R., and O'Connell R.J. (1982), Bulk attenuation in a polycrystalline Earth, *J. Geophys. Res. Solid Earth*, *87*, 7772–7778.
- Heinz D. and Jeanloz R. (1983), Inhomogeneity parameter of a homogeneous Earth, *Nature*, *301*, 138–139.
- Hirose K. and I. Kushiro(1993), Partial melting of dry peridotites at high pressures: Determination of compositions of melts segregated from peridotite using aggregates of diamond, *EPSL*, *114*, 477–489.
- Houser, C. and Q. Williams (2009), The relative wavelengths of fast and slow velocities in the lower mantle: Contrary to the expectations of dynamics? *Phys. Earth Planet. Int.*, *176*, 187–196.
- Hsu H., Blaha P., Cococcioni M. and Wentzcovitch R.M. (2011), Spin-state crossover and hyperfine interactions of ferric iron in MgSiO_3 perovskite, *Phys. Rev. Lett.*, *106*, 118501.
- Hsu H., Yonggang G.Y., and Wentzcovitch R.M. (2012), Spin crossover of iron in aluminous MgSiO_3 perovskite and post-perovskite, *EPSL*, *359*, 34–39.
- Irifune T., T. Shinmei, C. A. McCammon, N. Miyajima, D. C. Rubie, D. J. Frost (2010), Iron partitioning and density changes of pyrolite in Earth's lower mantle, *Science*, *327*, 193–195.

- Kawai K. and T. Tsuchiya (2014), P-V-T equation of state of cubic CaSiO_3 perovskite from first-principles computation, *J. Geophys. Res. Solid Earth*, *119*, 28012809, doi:10.1002/2013JB010905.
- Kawai K. and T. Tsuchiya (2015), Small shear modulus of cubic CaSiO_3 perovskite, *Geophys. Res. Lett.*, *42*, 27182726, doi:10.1002/2015GL063446.
- Kennett B.L.N., E.R. Engdahl, and R. Buland (1995), Constraints on seismic velocities in the Earth from traveltimes, *Geophys. J. Int.*, *122*, 108-124.
- Marquardt H., Speziale S., Reichmann H.J., Frost D.J., Schilling F.R., and Garnero E.J. (2009), Elastic shear anisotropy of ferropericlase in Earth's lower mantle, *Science*, *324*, 224-226.
- Masters G. (1979), Observational constraints on the chemical and thermal structure of the Earth's deep interior, *Geophys. J. Int.*, *57*, 507-534.
- Mattern E., Matas J., Ricard Y., and Bass J. (2005), Lower mantle composition and temperature from mineral physics and thermodynamic modelling, *Geophys. J. Inter.*, *160*, 973-990.
- Matyska C. and Yuen D.A. (2000), Profiles of the Bullen parameter from mantle convection modelling, *EPSL*, *178*, 39-46.
- Matyska C. and Yuen D.A. (2002), Bullens parameter η : a link between seismology and geodynamical modelling, *EPSL*, *198*, 471-483.
- McDonough W.F. and S.S. Sun (1995), The composition of the Earth, *Chem. Geo.*, *120*, 223-253, doi:10.1016/0009-2541(94)00140-4.

- Montagner J.P. and Kennett B.L.N. (1996), How to reconcile body-wave and normal-mode reference Earth models, *Geophys. J. Int.*, *125*, 229-248.
- Murakami, M., Y. Ohishi, N. Hirao, and K. Hirose (2012), A perovskitic lower mantle inferred from high-pressure, high-temperature sound velocity data, *Nature*, *485*, 90–94, doi:10.1038/nature11004.
- Piet H. ,J. Badro,F. Nabiei, T. Dennenwaldt, S. H. Shim, M. Cantoni, C. Hbert, and P. Gillet (2016), Spin and valence dependence of iron partitioning in Earth's deep mantle, *Proc. Natl. Acad. Sci.*, *113*, 11127-11130.
- Shukla, G., Z. Wu, H. Hsu, A. Floris, M. Cococcioni, and R. M. Wentzcovitch (2015), Thermoelasticity of Fe^{2+} -bearing bridgmanite, *Geophys. Res. Lett.*, *42*, 1741–1749.
- Shukla, G., M. Cococcioni, and R. M. Wentzcovitch (2016), Thermoelasticity of Fe^{3+} - and Al-bearing bridgmanite, *Geophys. Res. Lett.*, *43*, 56615670, doi:10.1002/2016GL069332.
- Shukla G. and R. M. Wentzcovitch (2016), Spin crossover in $(\text{Mg}, \text{Fe}^{3+})(\text{Si}, \text{Fe}^{3+})\text{O}_3$ bridgmanite: effects of disorder, iron concentration, and temperature, *Phys. Earth Planet. Int.*, Accepted, doi:doi:10.1016/j.pepi.2016.09.003.
- Speziale, S., A. Milner, V. E. Lee, S. M. Clark, M. P. Pasternak, and R. Jeanloz (2005), Iron spin transition in Earth's mantle, *Proc. Natl. Acad. Sci.*, *102*, 17918-17922.
- Stixrude, L. and C. Lithgow-Bertelloni (2005), Thermodynamics of mantle minerals I. Physical properties, *Geophys. J. Int.*, *162*, 610–632.
- Stixrude, L. and C. Lithgow-Bertelloni (2011), Thermodynamics of mantle minerals II. Phase equilibria, *Geophys. J. Int.*, *184*, 1180–1213.

- Tsuchiya, T., Wentzcovitch, R. M., da Silva, C. R., and de Gironcoli, S. (2006). Spin transition in magnesiowstite in Earth's lower mantle, *Phys. Rev. Lett.*, *96*, 198501.
- Valencia-Cardona J.J., G. Shukla, Z. Wu, C. Houser, D. Yuen, and R. M. Wentzcovitch (2017), Influence of the iron spin crossover in ferropericlase on the lower mantle geotherm, *Geophys. Res. Lett.*, *44*, 4863–4871. doi:10.1002/2017GL073294.
- Wentzcovitch R. M., B. B. Karki, M. Cococcioni, and S. de Gironcoli (2004), Thermoelastic properties of MgSiO_3 -Perovskite: Insights on the nature of the Earth's lower mantle, *Phys. Rev. Lett.*, *92*, 018501, doi:10.1103/PhysRevLett.92.018501.
- Wentzcovitch R. M., J. F. Justo, Z. Wu, C. R. S da Silva, D. A. Yuen, and D. Kohlstedt (2009), Anomalous compressibility of ferropericlase throughout the iron spin cross-over, *Proc. Natl. Acad. Sci.*, *106*, 8447-8452.
- Williams Q. and E. Knittle (2005), The uncertain major element bulk composition of Earth's mantle, *Earth's Deep Mantle: Structure, Composition, and Evolution. Geophysical Monograph Series 160. AGU*, doi:10.1029/160GM12.
- Wu Z., J. F. Justo, and R. M. Wentzcovitch (2013), Elastic anomalies in a spin-crossover system: Ferropericlase at lower mantle conditions, *Phys. Rev. Lett.*, *110*, 228501.
- Wu Z., J. F. Justo, C. R. S da Silva, S de Gironcoli, and R. M. Wentzcovitch (2009), Anomalous thermodynamic properties in ferropericlase throughout its spin crossover transition, *Phys. Rev. B.*, *80*, 014409.
- Wu Z., and R. M. Wentzcovitch (2014), Spin crossover in ferropericlase and velocity heterogeneities in the lower mantle, *Proc. Natl. Acad. Sci.*, *111*, 10468–10472.

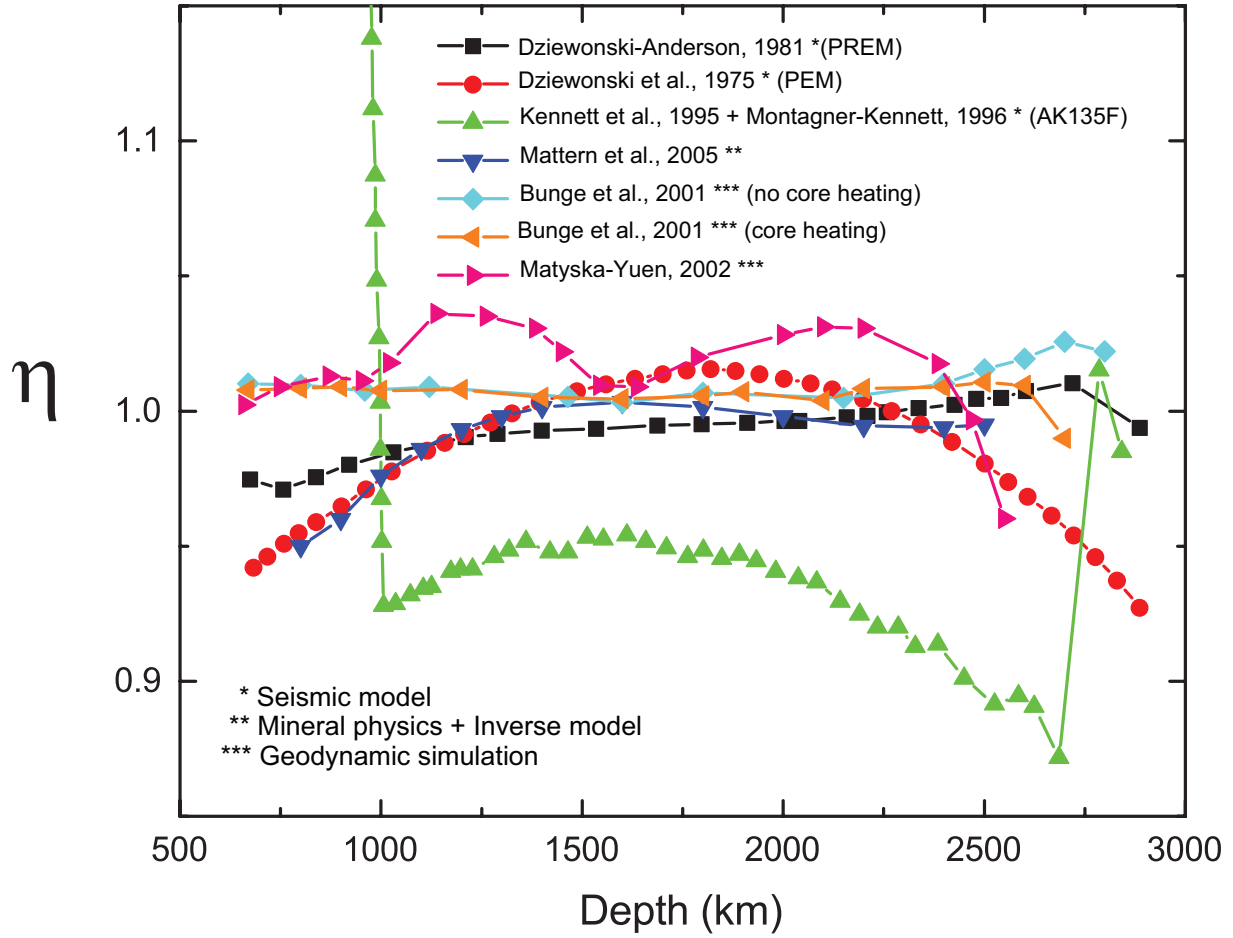


Figure 1. Bullen's parameter η calculations for seismic, geodynamic, and mineral physics models.

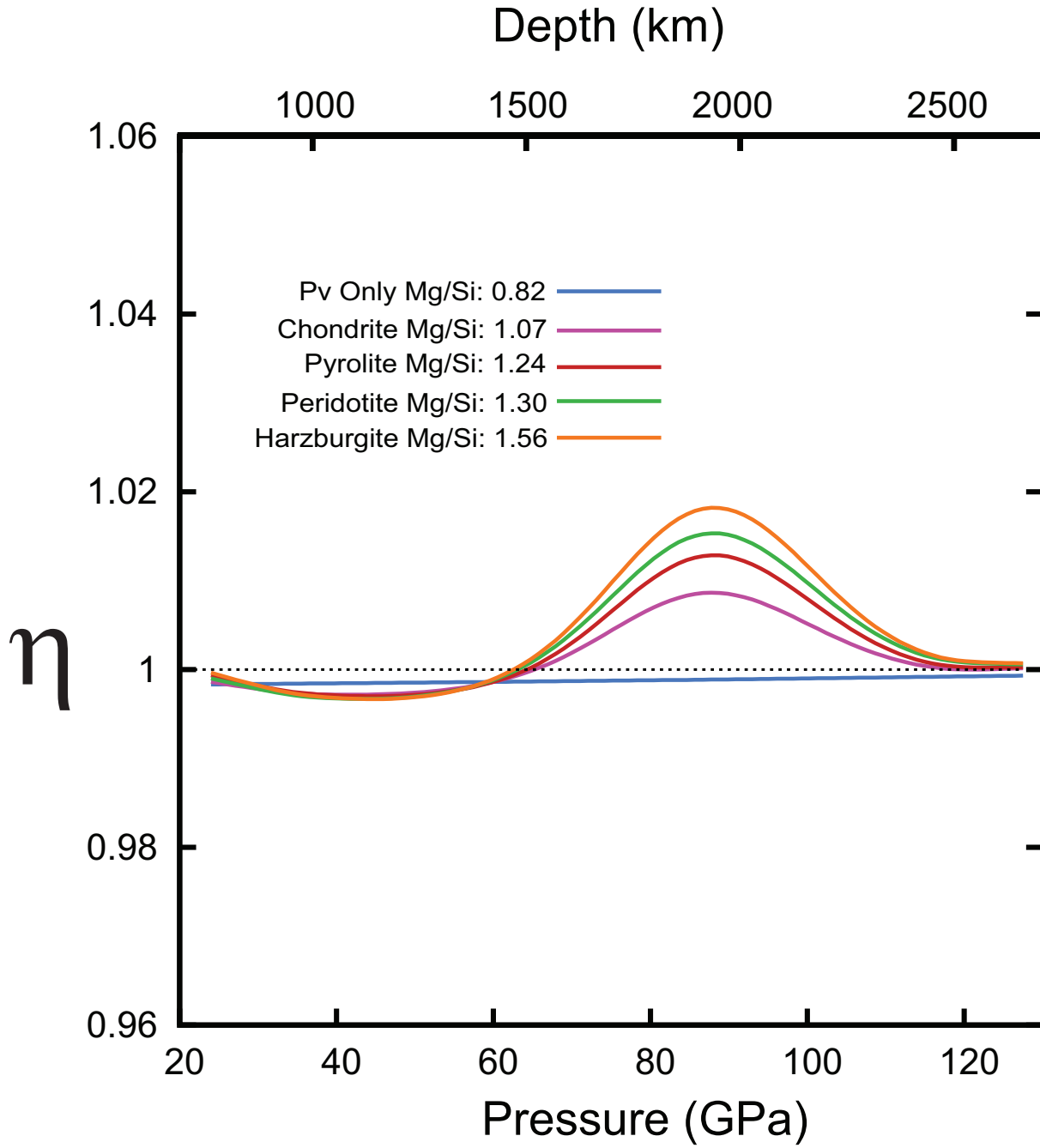


Figure 2. Perturbations of η due spin crossover in fp in lower mantle aggregates.

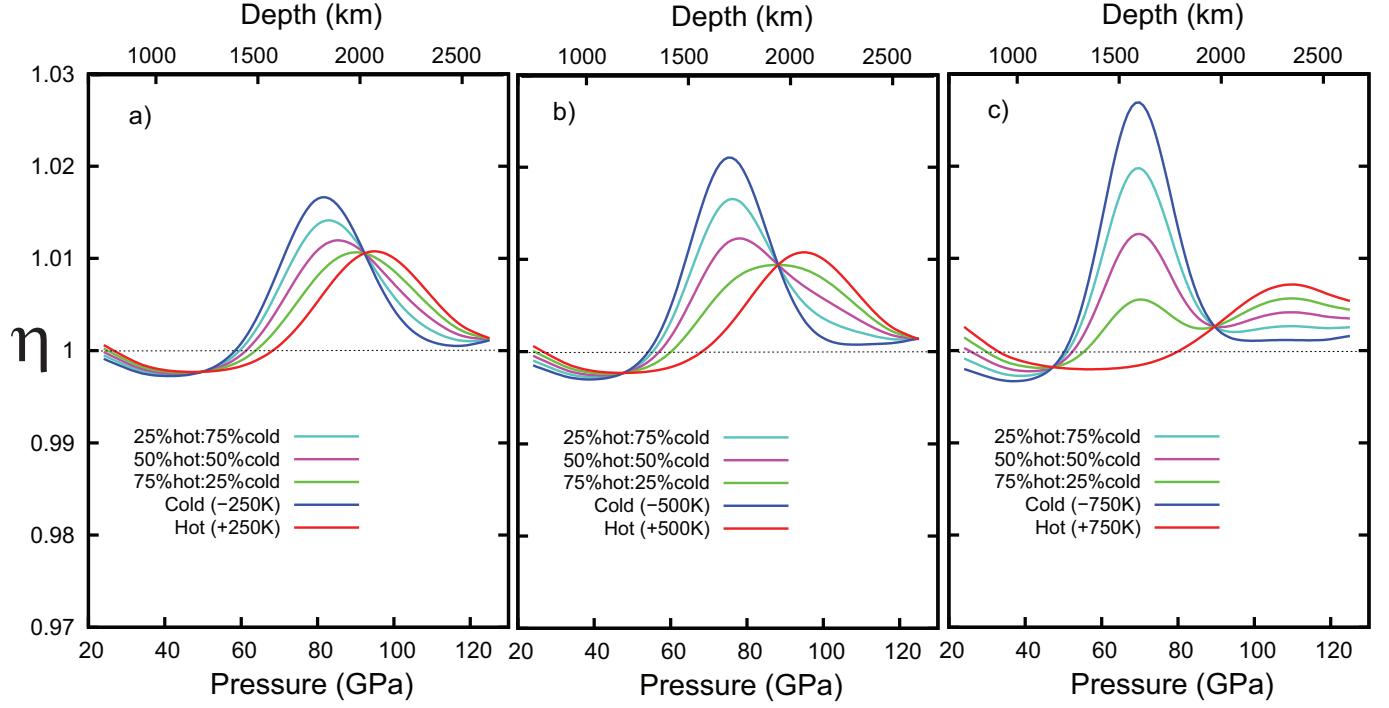


Figure 3. Lateral temperature variations of a) ± 250 K, b) ± 500 K, and c) ± 750 K for sequences of 25%:75%, 50%:50% and 75%:25% of the mantle being hot:cold.

In accord with the two-state model for temperature that we have assumed, two isosbestic points are generated near 1250 km and 2000 km depth, respectively.

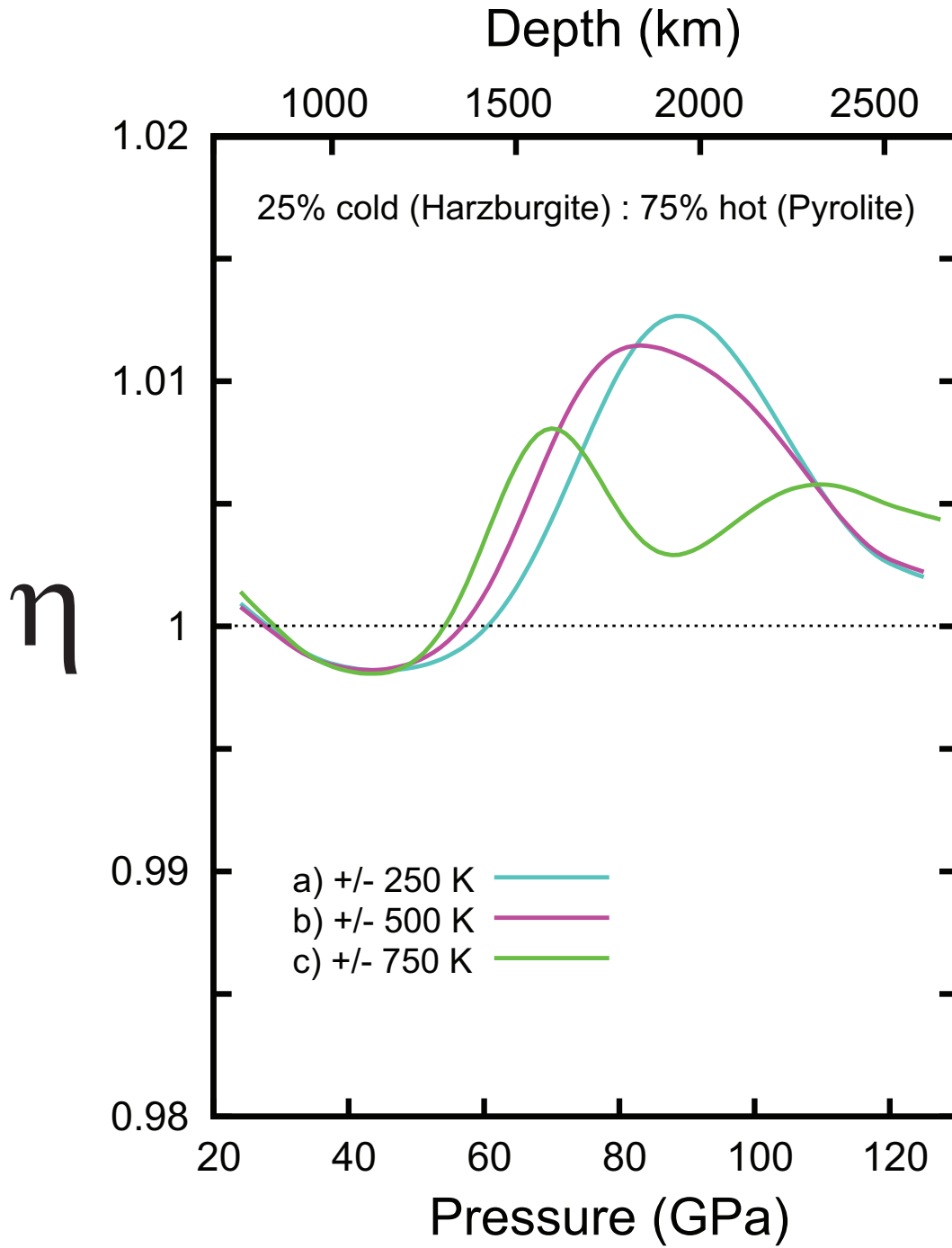


Figure 4. Lateral temperature and composition variations of a) ± 250 K, b) ± 500 K, and c) ± 750 K for a mantle being 25% cold(harzburgite): 75 % hot(pyrolite).

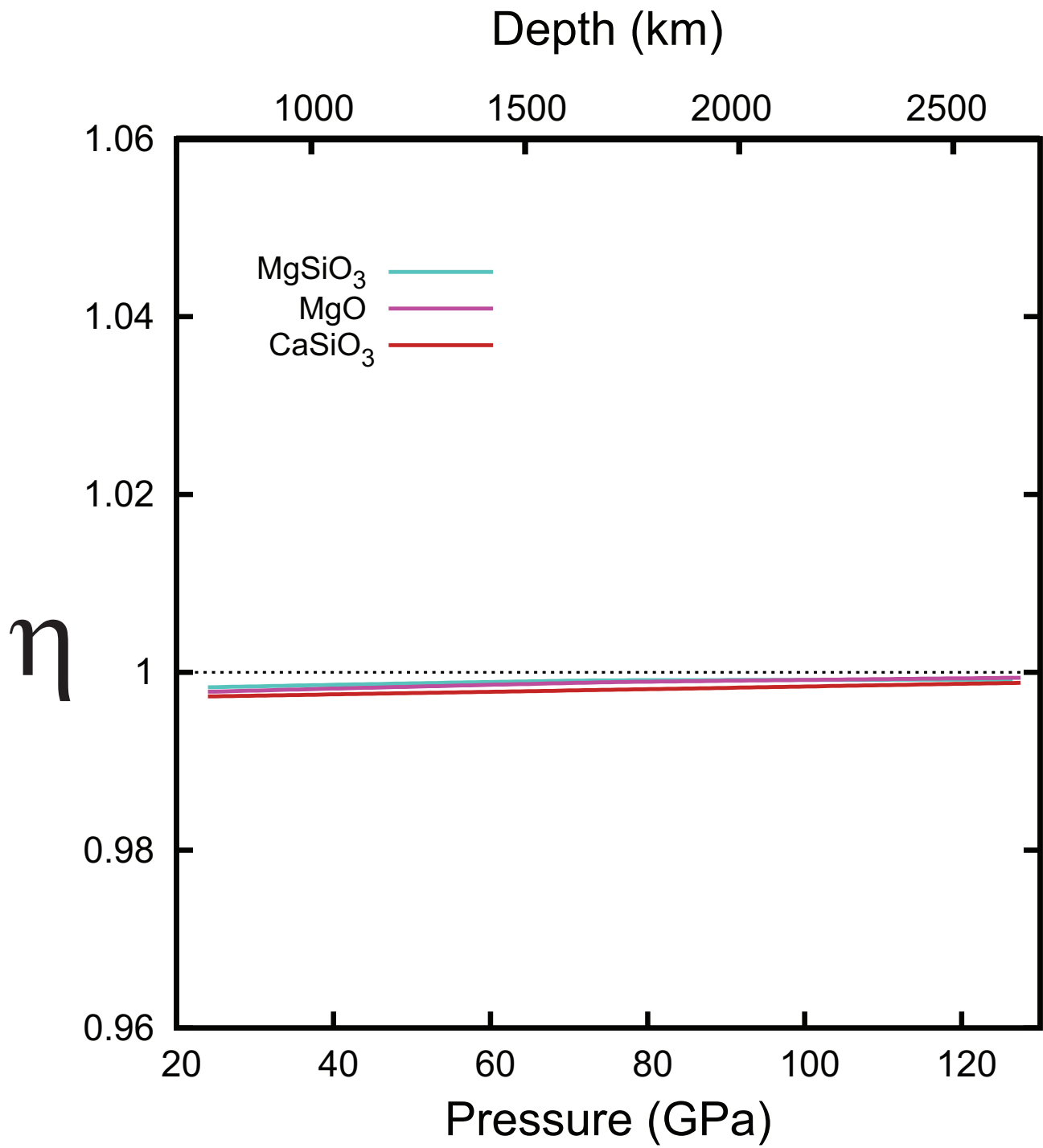


Figure S1. Bullen's parameter η for pristine lower mantle minerals.

Table 1. Bullen's parameter η for aggregates with fp in MS state.

Pressure (GPa)	Perovskite Only η	Chondritic η	Pyrolite η	Peridotite η	Harzburgite η
23	0.9983	0.9989	1.0008	0.9990	0.9996
30	0.9983	0.9981	0.9996	0.9978	0.9981
40	0.9984	0.9974	0.9985	0.9967	0.9967
50	0.9985	0.9976	0.9985	0.9968	0.9968
60	0.9986	0.9987	0.9998	0.9986	0.9987
70	0.9987	1.0020	1.0041	1.0038	1.0046
80	0.9987	1.0073	1.0116	1.0125	1.0148
90	0.9990	1.0091	1.0145	1.0157	1.0187
100	0.9990	1.0054	1.0092	1.0097	1.0117
110	0.9991	1.0016	1.0036	1.0032	1.0038
120	0.9992	1.0002	1.0016	1.0007	1.0009
125	0.9992	1.0003	1.0016	1.0006	1.0007